

## Supporting Information

### Effectively Exerting the Reinforcement of Dopamine Reduced Graphene Oxide on Epoxy-based Composites via Strengthened Interfacial Bonding

*Wenbin Li<sup>a,b,‡</sup>, Tinghua Shang<sup>a,‡</sup>, Wengang Yang<sup>a</sup>, Huichuan Yang<sup>a</sup>, Song Lin<sup>c</sup>,*

*Xiaolong Jia<sup>a,b,\*</sup>, Qing Cai<sup>a,\*</sup>, Xiaoping Yang<sup>a,b</sup>*

<sup>a</sup>State Key Laboratory of Organic-Inorganic Composites, College of Materials Science and Engineering, Beijing University of Chemical Technology, Beijing 100029, P. R. China, <sup>b</sup>Changzhou Institute of Advanced Materials, Beijing University of Chemical Technology, Jiangsu 213164, P. R. China, <sup>c</sup>Aerospace Research Institute of Materials and Processing Technology, Beijing 100076, China, <sup>‡</sup>contributed equally to the work.

E-mail: [jiaxl@mail.buct.edu.cn](mailto:jiaxl@mail.buct.edu.cn) & [caiqing@mail.buct.edu.cn](mailto:caiqing@mail.buct.edu.cn)

## Analysis of pDop-rGO

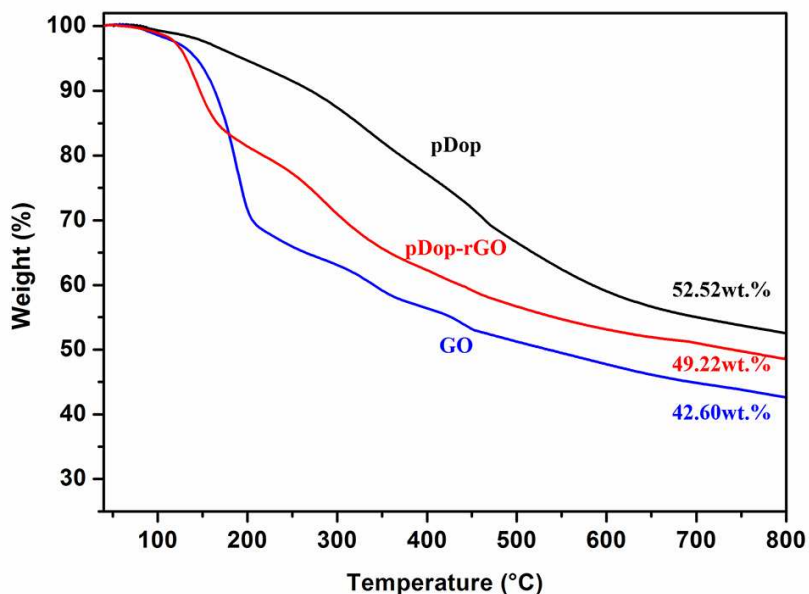


**Figure S1.** TGA curves of pDop, GO and pDop-rGO.

TGA measurements were conducted to evaluate the effect of pDop on the thermal stability of pDop-rGO. As shown in Figure S1, the rapid weight loss of GO around 180 °C indicated a large amount of oxygen-functional groups being decomposed at this temperature range.<sup>1</sup> The final weight loss of GO leveled off at ~60 %. Noticeably, pDop-rGO showed a rapid weight loss at the temperature of ~120 °C, and the leveled weight loss was ~50 %. In comparison with GO, the decomposition of pDop-rGO was able to occur at lower temperature because of the enhancement of chemical reduction on GO by pDop.<sup>1-2</sup> While the lower weight loss of pDop-rGO than that of GO was suggested as a result of the higher thermal stability of pDop. From Figure S1, the weight loss of pDop could be seen the smallest among the three samples, indicating its high carbon residue quantity upon heating in N<sub>2</sub> atmosphere. This feature might benefit from its structural similarity to phenolic resin.<sup>3</sup> Therefore, the weight loss of

pDop-rGO was reduced in comparison with that of GO due to the carbon-yielding characteristic of pDop. Moreover, the weight fraction of grafted pDop could be calculated from TGA data using the equation of  $Xf_{pDop} + (1-X)f_{GO} = f_{pDop-rGO}$ , where  $f_{pDop}$ ,  $f_{GO}$  and  $f_{pDop-rGO}$  are the weight loss fraction of pDop, GO and pDop-rGO, respectively, and  $X$  denotes the weight fraction of pDop in pDop-rGO.<sup>4-5</sup> The calculated weight fraction of pDop in pDop-rGO was ~66.7 wt.%.

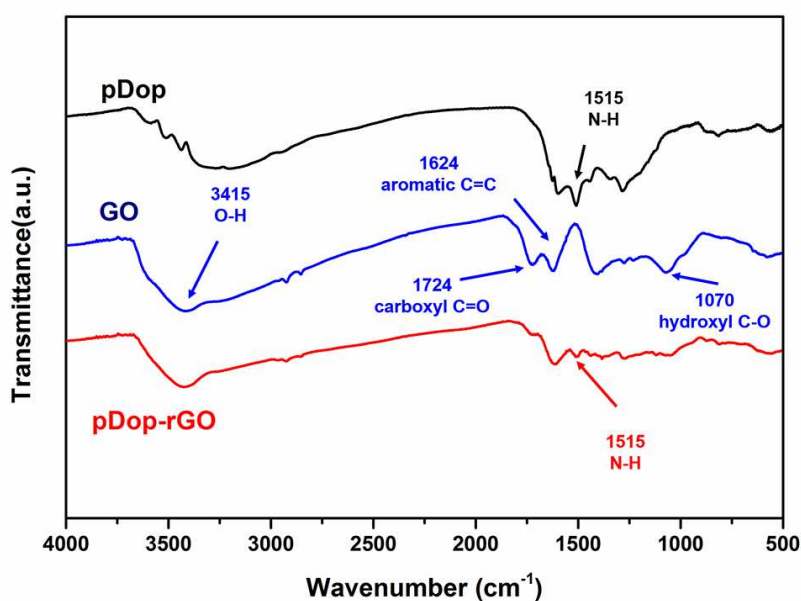


**Figure S2.** FT-IR spectra of pDop, GO and pDop-rGO.

Surface compositions of pDop-rGO were investigated by FT-IR. As shown in FT-IR spectra (Figure S2), the characteristic bands of GO were easily observed at 1070 (hydroxyl C-O stretching), 1624 (aromatic C=C stretching), 1724 (carboxyl C=O stretching), and 3415 cm⁻¹ (O-H stretching). Compared to the FT-IR spectrum of GO, the intensities of the two peaks at 1070 and 1724 cm⁻¹ decreased, while at the same time, a new absorption peak appeared at 1515 cm⁻¹ in the spectrum of pDop-rGO.

This new peak was corresponded to the N-H bending vibration from pDop as confirmed by the FT-IR spectrum of pDop. These facts suggested the successful incorporation of pDop component onto GO sheets.

### Kinetic parameters of different epoxy systems

**Table S1.** The calculated kinetic parameters for different epoxy systems.

Samples	Heating rate (°C /min)	$E_{\alpha}$ (KJ/mol)	n	m	lnA
EP	5	68.76	1.247	0.365	17.066
	10		1.193	0.378	17.047
	15		1.151	0.390	17.013
	20		1.127	0.394	16.980
EP+0.5 wt.% GO	5	73.42	1.343	0.356	18.110
	10		1.282	0.385	18.129
	15		1.248	0.367	18.082
	20		1.217	0.346	17.984
EP+0.5 wt.% pDop-rGO	5	66.25	1.248	0.388	16.484
	10		1.188	0.385	16.429
	15		1.171	0.418	16.443
	20		1.112	0.376	16.350

The kinetics parameters  $n$ ,  $m$  and  $\ln A$  were determined from each heating rate (5, 10, 15 and 20 °C /min), and their average values were used to determine the kinetics model. From all these calculations, the obtained results are listed in Table S1. Substituting the calculated kinetic parameters ( $E_{\alpha}$ ,  $n$ ,  $m$ , and  $\ln A$  in Table S1) into Equation (9), the explicit rate equations for the curing reaction of epoxy composites could be obtained.

## References

- (1) Lee, W.; Lee, J. U.; Jung, B. M.; Byun, J. H.; Yi, J. W.; Lee, S. B.; Kim, B. S. Simultaneous Enhancement of Mechanical, Electrical and Thermal Properties of Graphene Oxide Paper by Embedding Dopamine. *Carbon* **2013**, *65*, 296-304.
- (2) Moon, I. K.; Lee, J.; Ruoff, R. S.; Lee, H. Reduced Graphene Oxide by Chemical Graphitization. *Nat. Commun.* **2010**, *1*, 73-78.
- (3) Liu, R.; Mahurin, S. M.; Li, C.; Unocic, R. R.; Idrobo, J. C.; Gao, H.; Pennycook, S. J.; Dai, S. Dopamine as A Carbon Source: The Controlled Synthesis of Hollow Carbon Spheres and Yolk-Structured Carbon Nanocomposites. *Angew. Chem., Int. Ed.* **2011**, *50*, 6799-6802.
- (4) Jia, X. L.; Zheng, J. Y.; Lin, S.; Li, W. B.; Cai, Q.; Sui, G.; Yang, X. P. Highly Moisture-resistant Epoxy Composites: An Approach Based on Liquid Nano-Reinforcement Containing Well-dispersed Activated Montmorillonite. *RSC Adv.* **2015**, *5*, 44853-44864.
- (5) Jia, X. L.; Li, W. S.; Xu, X. J.; Li, W. B.; Cai, Q.; Yang, X. P. Numerical Characterization of Magnetically Aligned Multiwalled Carbon Nanotube-Fe<sub>3</sub>O<sub>4</sub> Nanoparticle Complex. *ACS Appl. Mater. Interfaces* **2015**, *7*, 3170-3179.